Liquid Crystals
Publication details, including instructions for authors and subscription information:
http://www.informaworld.com/smpp/title~content=t713926090

Calorimetric study of the cubic mesogen, ACBC(16)

Michio Sorai Corresponding author[a]; Kazuya Saito Corresponding author[a]; Tadahiro Nakamoto[a]; Mayumi Ikeda[a]; Yuri G. Galyametdinov[b]; Irina Galyametdinova[c]; Rudolf Eidenschink[d]; Wolfgang Haase[b]

[a] Research Center for Molecular Thermodynamics, Graduate School of Science, Osaka University, Osaka 560-0043, Japan [b] Institut für Physikalische Chemie, Fachgebiet Kondensierte Materie, Technische Universität Darmstadt, D-64287 Darmstadt, Germany [c] Kazan Physical-Technical Institute, Russian Academy of Sciences, 420029 Kazan, Russia [d] NEMATEL, D-55129 Mainz-Hechtsheim, Germany

Online publication date: 21 May 2010

To cite this Article Sorai Corresponding author, Michio , Saito Corresponding author, Kazuya , Nakamoto, Tadahiro , Ikeda, Mayumi , Galyametdinov, Yuri G. , Galyametdinova, Irina , Eidenschink, Rudolf and Haase, Wolfgang(2003) 'Calorimetric study of the cubic mesogen, ACBC(16)', Liquid Crystals, 30: 7, 861 — 869
To link to this Article: DOI: 10.1080/0267829031000121206
URL: http://dx.doi.org/10.1080/0267829031000121206

LIQUID CRYSTALS, VOL. 30, NO. 7, JULY, 2003, 861–869

Calorimetric study of the cubic mesogen, ACBC(16)§

MICHIO SORAI*, KAZUYA SAITO*, TADAHIRO NAKAMOTO, MAYUMI IKEDA

Research Center for Molecular Thermodynamics, Graduate School of Science, Osaka University, Toyonaka, Osaka 560-0043, Japan

YURI G. GALYAMETDINOV, IRINA GALYAMETDINOVA

Institut für Physikalische Chemie, Fachgebiet Kondensierte Materie, Technische Universität Darmstadt, Petersenstrasse 20, D-64287 Darmstadt, Germany; Kazan Physical-Technical Institute, Russian Academy of Sciences, Sibirsky Tract 10/7, 420029 Kazan, Russia

RUDOLF EIDENSCHINK

NEMATEL, Galileo-Galilei Strasse 28, D-55129 Mainz-Hechtsheim, Germany

and WOLFGANG HAASE

Institut für Physikalische Chemie, Fachgebiet Kondensierte Materie, Technische Universität Darmstadt, Petersenstrasse 20, D-64287 Darmstadt, Germany

(*Received 31 January 2003; accepted 10 March 2003*)

The heat capacity of the cubic mesogen ACBC(16) was measured between 16 and 500 K by adiabatic calorimetry. As well as the known condensed phases, a new crystalline phase was found to undergo a glass transition at around 165 K. Phase transitions between crystal, SmC, cubic, and isotropic liquid phases took place at 399.16, 431.15, and 474.30 K, respectively. As in the case of ANBC, a broad hump was observed in the heat capacity of the isotropic liquid phase. The first order nature of the SmC–cubic phase transition was confirmed for the first time by the observation of supercooling of the cubic phase. The broad hump in the isotropic liquid phase was shown to extend to a low temperature side if the isotropic liquid was supercooled, suggesting that the event occurring at the hump is not directly related to the cubic–isotropic liquid phase transition.

1. Introduction

It is widely believed that optically isotropic (cubic) mesogens have little application potential because optical anisotropy plays the primary role in the applications of liquid crystals. However, isotropic liquid crystals, in which 'rod-like' molecules having a large structural anisotropy form a higher order isotropic structure by aggregation, provide very interesting and challenging issues, to our understanding of the condensation mechanisms of molecules.

In previous papers on thermotropic cubic mesophases [1–7], we presented an experimental basis for treating many (effectively, most) real thermotropic liquid crystals as a binary system consisting of the 'molecular core,' i.e. the central part of a molecule, and alkyl chain(s). Chains are highly disordered in liquid crystalline phases and serve as an 'intramolecular solvent' or 'self-solvent' [2–4, 6, 7]. Based on such a quasi-binary picture, the alkyl chain length dependence of the entropy of transition between the SmC phase and cubic mesophase in the ANBC(n) (4′-n-alkoxy-3′-nitrobiphenyl-4-carboxylic acid, n: the number of carbon atoms in the alkoxy chain, figure 1) and BABH(n) (1,2-bis(4-n-octyloxybenzoyl)hydrazine) series was analysed to show that the core is more ordered while the chain is more disordered in cubic phases [4, 6]. That is, there is an entropic competition between the core and chain.

*Authors for correspondence;
e-mail: sorai@chem.sci.osaka-u.ac.jp
e-mail: kazuya@chem.sci.osaka-u.ac.jp

§Contribution No. 74 from the Research Center for Molecular Thermodynamics.

Liquid Crystals ISSN 0267-8292 print/ISSN 1366-5855 online © 2003 Taylor & Francis Ltd
http://www.tandf.co.uk/journals
DOI: 10.1080/0267829031000121206

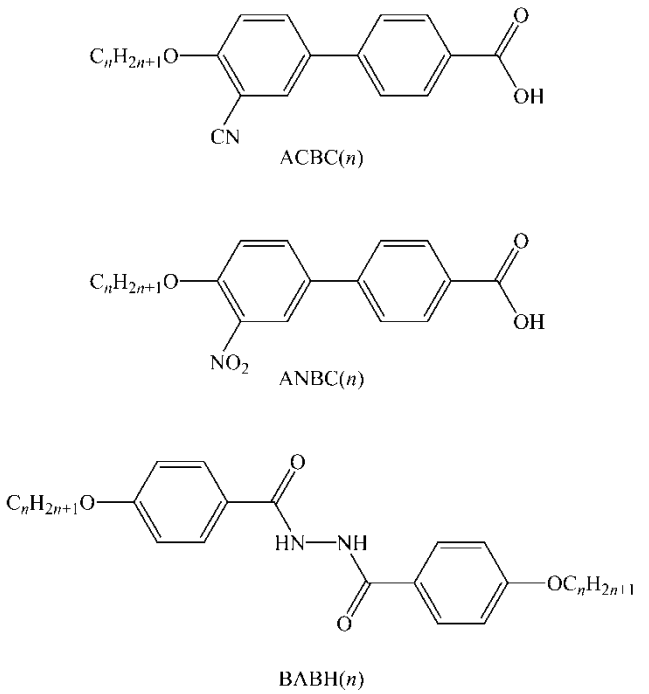

Figure 1. Molecular structures of the classical cubic mesogens, ACBC(*n*), ANBC(*n*) and BABH(*n*), where *n* is the number of carbon atoms in the alkyl chain.

The title compound, ACBC(*n*) (4′-*n*-alkoxy-3′-cyanobiphenyl-4-carboxylic acid, figure 1) [8], forms a group of classical cubic mesogens together with ANBC(*n*) [8–10] and BABH(*n*) [11, 12]. Although ANBC [1, 3, 4, 6, 13–21] and BABH [2, 22] have been widely and extensively investigated, studies on ACBC [8, 15, 23, 24] have been scarce, probably owing to the difficulty of sample preparation. The most interesting point is that the space group of the cubic phase is *Im*3*m* in ACBC(18) [8, 15] but *Ia*3*d* in ANBC(18) [15] in spite of the close resemblance of the molecules (see figure 1). In the case of $n=16$, the transition temperatures:

ACBC(16) [12]:

$$\text{crystal} \xrightarrow{399.16\text{K}} \text{SmC} \xrightarrow{431.15\text{K}} \text{cubic (?)} \xrightarrow{474.30\text{K}} \text{isotropic liquid (I)}$$

ANBC(16) [3]:

$$\text{crystal} \xrightarrow{401.12\text{K}} \text{SmC} \xrightarrow{445.95\text{K}} \text{cubic (I}a3d\text{)} \xrightarrow{470.80\text{K}} \text{SmA} \xrightarrow{472.04\text{K}} \text{I}$$

According to previous work, ANBC(22) exhibits two isotropic mesophases with the space groups *Im*3*m* and *Ia*3*d* on heating [6, 18, 20]; the appearance of the *Im*3*m* phase for ACBC(16) would be expected as a result of weaker lateral interactions in ACBC than in ANBC assuming the same effective core size for the two compounds. The lower SmC–cubic transition temperature seems to be consistent with the explanation. In the present paper, the thermodynamic properties of a historically important cubic mesogen, ACBC(16), are described in detail.

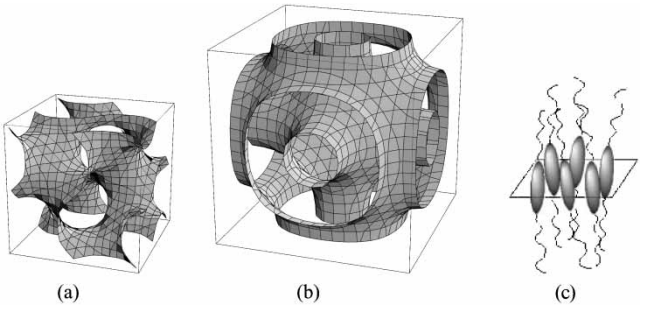

Figure 2. Structural models of unit cells of the cubic (*a*) *Ia*3*d* and (*b*) *Im*3*m* phases of ANBC and ACBC. (*c*) Cores of carboxylic acid dimers are on the surface (TPMS) and on average are perpendicularly oriented with respect to the surface.

Recently a full application of the quasi-binary picture of thermotropic liquid crystals to cubic mesophases in classical cubic mesogens was made [25] to construct structural models. Thus, mesogenic cores aggregate by intermolecular interactions in lateral directions to form a sheet. The two-side symmetry arising from the 'doubled structure' of mesogens requires that the mean curvature of the sheet vanishes, resulting in a 'minimal surface' [26]. Their experimentally determined space groups and relative dimensions of the unit cells select uniquely a combination of possible structures characterized by triply periodic minimal surfaces (TPMS) as shown in figure 2 [25]. The new experimental results on ACBC(16) will also be discussed in relation to this structural model.

2. Experimental

ACBC(16) was synthesized at Technische Universität Darmstadt according to the scheme [27, 28]. The yellowish polycrystals were bleached by repeated recrystallization from a hot ethanol suspension of charcoal and then dried in a vacuum. The quality of the specimen

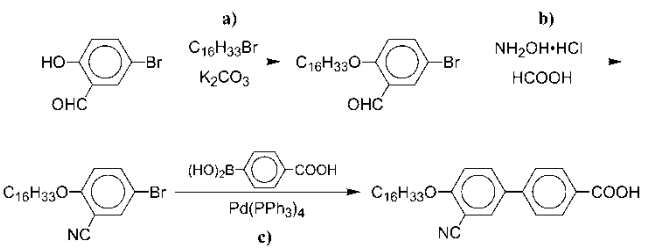

Scheme. a) Reflux in ethanol for 24 h; b) reflux for 6 h according to [27]; c) reflux in toluene for 24 h according to [28].

was checked by elemental analysis: found, C 77.47, H 8.94, N 3.04; calcd. for $C_{30}H_{41}O_3N$, C 77.71, H 8.91, N 3.02%.

The phase behaviour of ACBC(16) was preliminarily examined using a differential scanning calorimeter (Perkin Elmer: Pyris-1 DSC) prior to precise heat capacity measurements. Optical textures were observed using a polarizing microscope (Olympus, LK-982) with a computer-controlled heating/cooling stage (Japan High-tech Co).

Heat capacity measurements were made between 16 and 500 K by use of a home-built adiabatic calorimeter [29]. The heat capacities above room temperature were measured twice by using different specimens from the same batch of sample. The mass of the specimen used for the calorimetry was 2.15490 g (4.64759 mmol) for the first series (A) of measurements and 2.21379 g (4.77460 mmol) for the second (B). The sample was loaded into a quartz glass beaker with a lid (5.7 g in mass), to avoid direct contact between the sample and the wall of the gold-plated copper–beryllium vessel. The beaker was placed in the vessel and sealed after introducing a small amount of helium gas (23 kPa at room temperature) to assist thermal equilibration inside the vessel. Mounted on the calorimeter vessel was a platinum resistance thermometer (Minco Product, S1055), whose temperature scale is based upon the IPTS-68. The contribution of the sample was more than 20% of the total heat capacity including those of the vessel and the glass beaker. The details of the adiabatic calorimeter, the operation and procedure of heat capacity measurements are described elsewhere [29].

ACBC(16) decomposed slightly in the measurement by adiabatic calorimetry because of long exposure to high temperatures. Inspection of the samples after heat capacity measurements [2–4, 6], however, suggested that the decomposition of the present compound was sluggish compared with that of BABH(8) and ANBC(*n*). The heat capacity measurement for sample B mainly focused on the observation of the supercooling phenomena of the SmC – cubic and clearing transitions, which were believed to be first order in nature, for the first time because of the fairly good thermal stability of ACBC(16).

3. Results and discussion

3.1. *Differential scanning calorimetry*

The results of the preliminary DSC experiments are schematically summarized in figure 3. In the first heating run at a rate of 2 K min^{-1}, ACBC(16) exhibited a large endothermic peak at 388 K and a small peak at 399 K. The microscopic observation showed that the latter endotherm corresponds to the melting to the SmC phase. On further heating, the sample underwent

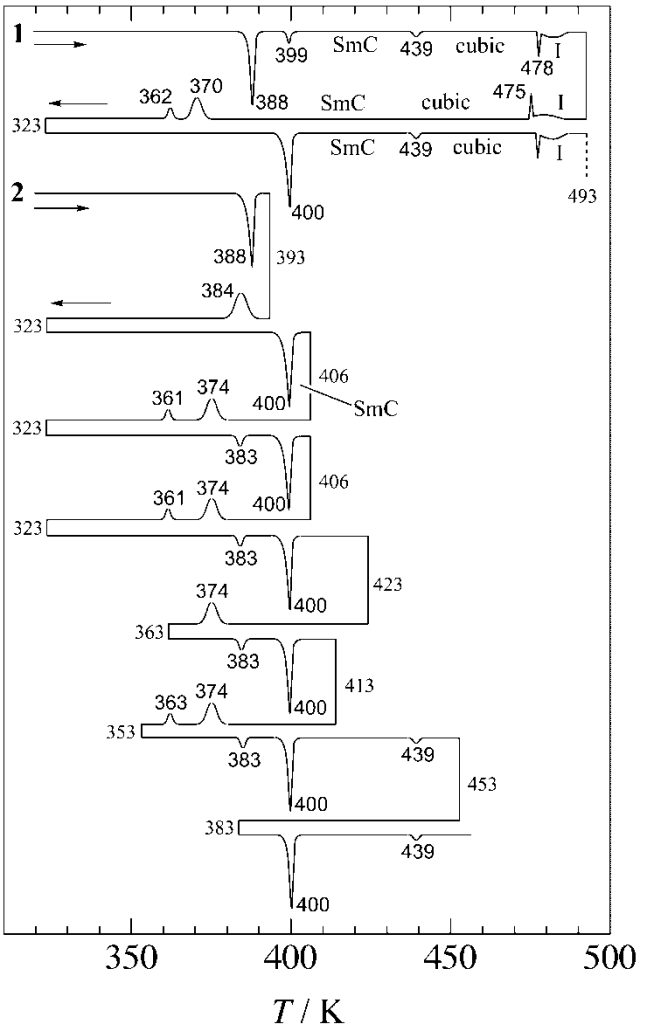

Figure 3. Summary of DSC experiments on ACBC(16).

a phase transition to the cubic phase at around 439 K and a clearing transition at around 478 K. Just after the sharp endothermic peak due to the clearing, a broad hump was observed. In a subsequent cooling run, a broad hump and an exothermic peak appeared at lower temperatures than those in the heating run. The cubic → SmC phase transition was not detected in this cooling process though the microscopic observation implied that the transition probably occurred above room temperature during cooling. On further cooling, two exothermic peaks were observed at around 370 and 362 K, neither of which seemed to correspond to the two phase transitions in the crystalline states detected in the first heating run, as judged from their associated enthalpies. The resulting solid, on heating, exhibited a single endothermic peak at around 400 K, above which the sample was in the SmC phase.

To get more insight into the complicated phase

behaviour of ACBC(16), the experiments were repeated extensively as shown in the lower part of figure 2. A consistent phase relationship (or equivalently, a temperature–Gibbs energy diagram) could be constructed to account for the DSC results. The equilibrium measurements performed by adiabatic calorimetry, however, showed that the correct phase relationship was more complicated than that revealed by DSC. The essential conclusions from these DSC experiments relevant here are: (i) there are multiple crystalline phases below the melting temperature; (ii) their thermodynamic relationship is very complex; (iii) despite such complexity for the crystalline phases, the phase behaviour is simple for the liquid crystalline and isotropic liquid phases including the cubic mesophase.

3.2. *General results of adiabatic calorimetry*

The heat capacity of ACBC(16) was measured between 16 and 500 K. Typical data are shown in figure 4 for the whole temperature range studied. Strictly speaking, a correction for the heat of sublimation and vaporization of the sample into the free space of the calorimeter vessel should be made to the heat capacities at high temperatures. However, this correction was neglected because the free space in the vessel was small and the vapor pressure of ACBC(16) is very low as indicated by the absence of weight loss during the drying of the sample under vacuum.

The first series of heat capacity measurements for the as-grown sample (sample A) is indicated by open circles in figure 4. Three crystalline phases (C_3, C_2, C_1), two mesophases (SmC, cubic), and the isotropic liquid phase (I) were observed (see also figure 5). The transition temperatures were determined to be 385.67 K (C_3–C_2), 397.20 K (C_2–C_1), 399.16 K (C_1–SmC), 431.15 K (SmC–cubic) and 474.30 K (cubic–I).

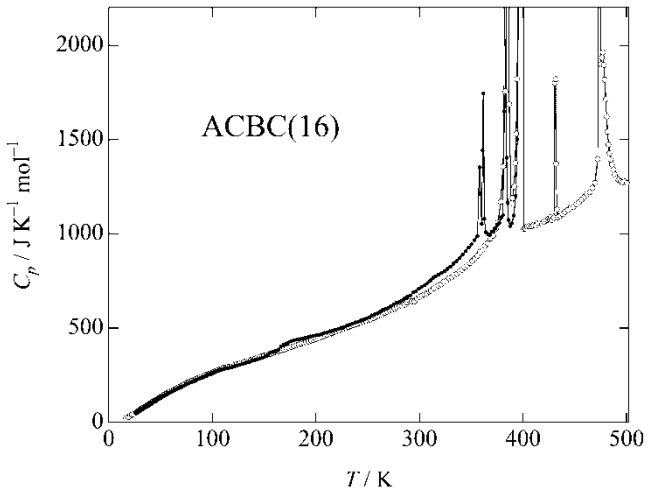

Figure 4. Measured heat capacities of ACBC(16). Open circles are for the as-grown sample and closed circles for the sample crystallized from SmC phase.

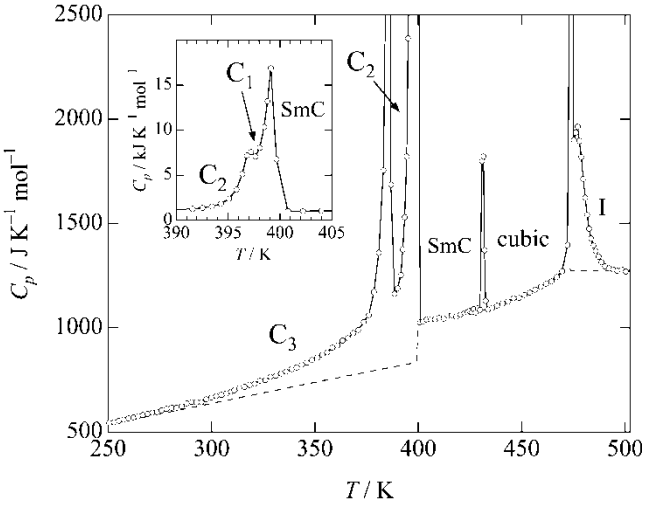

Figure 5. Measured heat capacities and assumed normal heat capacities (dashed lines) of ACBC(16).

It should be noted here that a very weak heat evolution occurred during the temperature drift measures at around 390 K. This heat evolution might be thought to have some connection with the transition from a metastable to a stable phase. After annealing, the sample was cooled below room temperature in order to obtain the 'stable' crystalline phase, and then the heat capacity measurement was started from just below the phase transition at 385.67 K. The phase transition at 385.67 K never vanished, in contrast to the DSC results described in the preceding section. The results depended on the observation method because of kinetic problems. The heat capacity measurements performed by confirming the thermal equilibrium of the sample are more reliable for the determination of the stable phase relationships than the DSC measurement performed using a fast temperature scan before equilibrium is reached.

After cooling from the SmC phase, the measurements at low temperatures yielded the data indicated by filled circles. The sample was found to exhibit a new crystalline phase and underwent a glass transition at around 170 K. Above this glass transition temperature, the heat capacities became remarkably larger than these of the as-grown crystalline sample and exhibited two weak sharp peaks at 358.1 and 361.7 K. At temperatures above these peaks, the heat capacity became similar to that of the as-grown crystalline sample. This sample also showed two large thermal anomalies at 387.0 and 399.6 K; these temperatures are very close to those of

the C_3–C_2 and C_1–SmC transitions of the as-grown sample, respectively. The heat capacity data of the two series agreed well above the SmC phase, and were compatible with the DSC results. The numerical data for the heat capacity above the melting temperature are listed in table 1.

To discuss the thermodynamic properties of transitions such as excess enthalpy and entropy, separation of the excess part of the heat capacity is necessary. When a transition is first order in nature, the normal heat capacity may jump at the transition temperature. It is, however, often hard to draw such a baseline for each phase. In the present case, a jump in the heat capacity due to different baselines is clearly seen for the transition at 399.1 K. The baseline of the heat capacity below this temperature, i.e. in phases C_3, C_2 and C_1, was determined by using the effective frequency distribution method [30]. The resulting normal heat capacity is shown by a dashed curve in figure 5. For the SmC and cubic phases, the heat capacities were fitted to the quadratic polynomials,

$$C_p(\mathrm{SmC})/\mathrm{J\,K^{-1}\,mol^{-1}} = 3236.8 - 12.549(T/\mathrm{K}) + 1.7566\times10^{-2}(T/\mathrm{K})^2 \quad (399 < T/\mathrm{K} < 430)$$

$$C_p(\mathrm{cubic})/\mathrm{J\,K^{-1}\,mol^{-1}} = 1004.6 - 44.119(T/\mathrm{K}) + 5.4119\times10^{-2}(T/\mathrm{K})^2 \quad (433 < T/\mathrm{K} < 470)$$

The excess heat capacities thus separated from the observed heat capacities were integrated numerically to

Table 1. Measured molar heat capacities of ACBC(16) above the melting temperature. Series A and B correspond to the measurements for freshly loaded different specimens from an identical batch of sample.

T	C_p	T	C_p	T	C_p	T	C_p
K	$\mathrm{J\,K^{-1}\,mol^{-1}}$	K	$\mathrm{J\,K^{-1}\,mol^{-1}}$	K	$\mathrm{J\,K^{-1}\,mol^{-1}}$	K	$\mathrm{J\,K^{-1}\,mol^{-1}}$
	Series A1	461.763	1211.5	420.233	1063.2	463.973	1210.7
400.756	1025.7	464.363	1221.5	422.232	1071.1	465.901	1226.0
402.210	1028.9	466.954	1243.2	424.230	1078.9	468.303	1248.5
403.998	1039.6	469.532	1270.7	426.224	1082.8	470.696	1279.4
406.043	1040.4	472.070	1396.2	427.717	1093.0	472.363	1296.2
408.086	1040.3	473.685	3443.4	428.710	1083.6	473.459	2597.0
410.125	1047.7	474.388	3962.9	429.702	1093.5	474.156	3802.4
412.161	1042.7	475.186	1899.4	430.683	1174.4	474.837	2881.9
414.196	1058.2	476.092	1935.7	431.381	2000.1		
416.227	1059.9	476.990	1963.4	431.802	1935.0		Series B3
418.256	1053.1	477.891	1895.0	432.242	1512.3	471.491	1604.4
420.283	1063.1	478.794	1818.1	432.706	1356.8	472.472	1673.7
422.300	1069.4	479.710	1714.0	433.183	1218.1	473.433	1730.4
423.811	1074.1	480.636	1623.2	433.673	1086.7	474.373	1793.5
424.816	1080.2	481.573	1541.5	434.410	1083.1	475.298	1811.0
425.819	1075.8	482.520	1474.6			476.213	1842.8
426.819	1089.1	483.473	1427.5		Series B2	477.122	1797.9
427.820	1072.9	484.556	1393.7	428.180	1058.8	478.030	1711.8
428.820	1092.7	485.772	1367.9	429.177	1070.2	479.205	1598.8
429.816	1086.4	487.123	1340.4	430.171	1065.3	480.652	1496.5
430.748	1800.0	488.600	1313.7	431.163	1077.1	482.124	1465.9
431.428	1820.8	490.276	1294.6	432.153	1073.5	483.626	1399.0
431.932	1372.5	492.211	1285.3	433.143	1084.0	485.134	1338.8
432.468	1129.2	494.215	1279.5	434.628	1084.4	486.657	1326.2
433.732	1087.5	496.229	1273.8	436.607	1090.0	488.185	1311.5
435.721	1094.9	498.246	1278.6	438.583	1096.0	489.723	1293.3
438.046	1105.5	500.266	1270.3	440.555	1105.0	491.266	1277.9
440.706	1116.0	502.289	1274.3	442.522	1113.6	492.815	1281.8
443.359	1126.2			444.979	1119.7	494.628	1278.9
446.006	1142.1		Series B1	447.921	1129.4	496.706	1263.0
448.649	1142.6	410.580	1055.3	450.856	1144.9	498.785	1268.4
451.286	1156.5	412.193	1049.5	453.784	1153.9	501.128	1256.2
453.915	1168.4	414.209	1054.4	456.707	1168.2	503.733	1268.0
456.538	1182.4	416.220	1058.5	459.621	1184.0		
459.153	1196.6	418.228	1063.8	462.043	1197.6		

Table 2. Thermodynamic properties of phase transitions in ACBC(16).

	T	ΔH	ΔS
	K	$J K^{-1} mol^{-1}$	$J K^{-1} mol^{-1}$
$C_3 \rightarrow C_2$	385.67	26.34	71.63
$C_2 \rightarrow C_1$	397.20	14.98	37.87
$C_1 \rightarrow$SmC	399.16	21.64	54.25
SmC→cubic	431.15	1.15	2.67
Cubic→I[a]	474.30	3.96	8.36
Hump in I	477[b]	4.4	9.2

[a] Isotropic liquid.
[b] Temperature of the maximum.

yield the excess enthalpy and entropy. The numerical data are summarized in table 2 for the phase transitions. It is difficult to discuss, at present, the properties of each phase transition between the crystalline phases because information concerning the crystal structures and molecular dynamics in each phase is not available.

3.3. *Heat capacity of liquid crystalline phases*

Although the heat capacity of ACBC(16) is noticeably different from that of ANBC(16) [3] in the crystalline phases, they become practically identical in the liquid crystalline phases as seen in figure 6. This fact can be basically understood, as the motional disorder of alkyl chains is equally excited in the two compounds in the liquid crystalline phases.

In previous papers [3, 4, 6], we pointed out that the cubic mesophases have a smaller heat capacity than the neighbouring liquid crystalline phases, as shown in figure 6 for ANBC(16) [3]. This trend also holds for ACBC(16). In figure 7, the two sets of heat capacity data obtained for independent series (using the samples A and B) are plotted using open circles and crosses. A small systematic difference can be seen and should give an estimate of the accuracy (and reproducibility) of the present experiment. The precision of the measurements is better than the accuracy as seen from the figure. The data plotted using open circles shows that the heat capacity of the cubic phase is smaller than that of the SmC phase if they are compared at the same temperature.

Similar behaviour is observed in lyotropic cubic mesophase [31]. Heat capacity (under constant pressure) is proportional to the mean squared amplitude of enthalpy fluctuation. The cubic mesophases considered have three-dimensional periodicity resulting from three-dimensional connectivity of a structural motif (sheet or rods). This connectivity will suppress the fluctuation.

3.4. *SmC–cubic phase transition*

Figure 7 shows the molar heat capacities around the SmC to cubic phase transition. The data plotted using crosses were obtained from the run using sample B heated to 435 K and then cooled to 428 K. The data

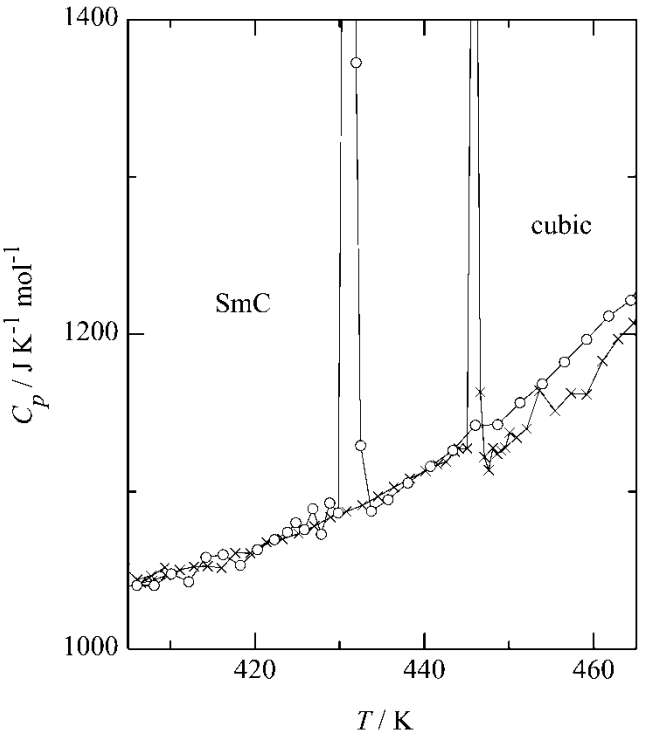

Figure 6. Comparison of heat capacities between ACBC(16) (circle) and ANBC(16) (cross).

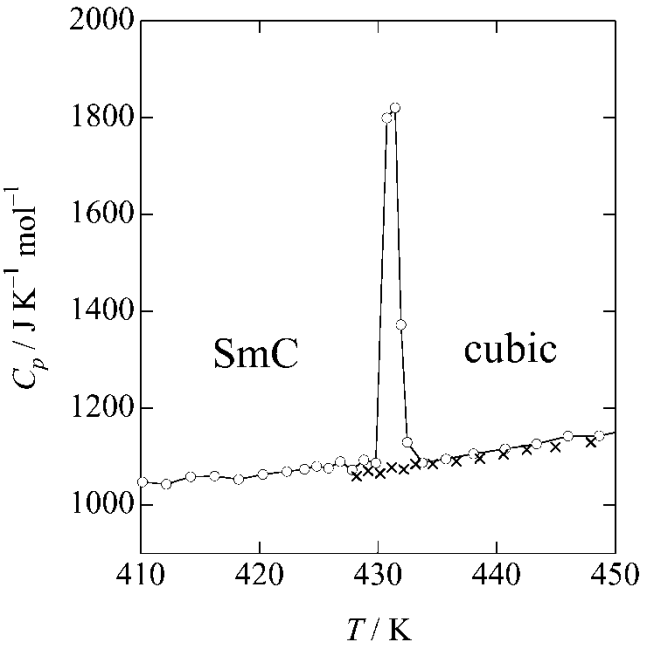

Figure 7. SmC–cubic phase transition of ACBC(16). Crosses show the results after cooling from the cubic phase to slightly below the transition temperature.

show no sign of the SmC – cubic transition at around 431.15 K, indicating a successful supercooling of the cubic phase as a thermodynamic equilibrium (though metastable) state. This is the first concrete evidence of the first order nature of the SmC – cubic phase transition in classical cubic mesogens studied thermodynamically—BABH(8), ANBC(n) ($n=16$, 18, 22) and the present ACBC(16) [2–4, 6].

We have shown that the analysis of the chain length dependence of the entropy of transition gives crucial information clarifying the aggregation states [4, 6, 32]. In particular, based upon the experimental results for the ANBC series and the expected magnitude of the dipole moments of nitro and cyano groups, the data suggested that the appearance of an *Im*3*m* phase in ACBC(16), instead of the *Ia*3*d* phase in ANBC(16), is favored because of the weaker intermolecular interactions in the lateral direction in ACBC(16) than in ANBC(16), if the core size of ACBC(16) is the same as that of ANBC(16) [6].

The entropy of the SmC – cubic transition of ACBC(16) is larger than that of ANBC(16) ($1.63\,J\,K^{-1}\,mol^{-1}$) [3]. If the entropy contribution of the core, which was assumed to depend primarily on the effective core size [4, 6], is identical in two compounds, the chain length dependence of the entropy of transition is also expected to be identical. However, this assumption is probably too specific to apply for different series of compounds, even though the molecular structures of ACBC and ANBC are similar. To extend the discussion further, therefore, structural information of the cubic phase of ACBC(16) is required. Experiments are now under way in collaboration with Prof. Kutsumizu at Gifu University [33].

3.5. *Heat capacity hump in the isotropic liquid*

A broad hump was observed just above the transition to the isotropic liquid at 474.30 K in the heat capacity curve as shown in figure 8 on an enlarged scale. This hump was also observed in DSC experiments. Although the temperatures of both the sharp peak and the hump depended on the direction of the temperature change, they appeared to remain at a similar relative position as seen in figure 3. This observation may lead to the possible explanation that the cubic–I transition intrinsically accompanies a broad peak. This is however not the case. The data plotted using crosses in figure 8 are those obtained after cooling from the temperature of the top of the hump to below the cubic–I transition temperature. The broad hump extends below the transition. This clearly excludes this possible explanation.

Similar broad humps have been reported for some liquid crystalline substances at temperatures above the

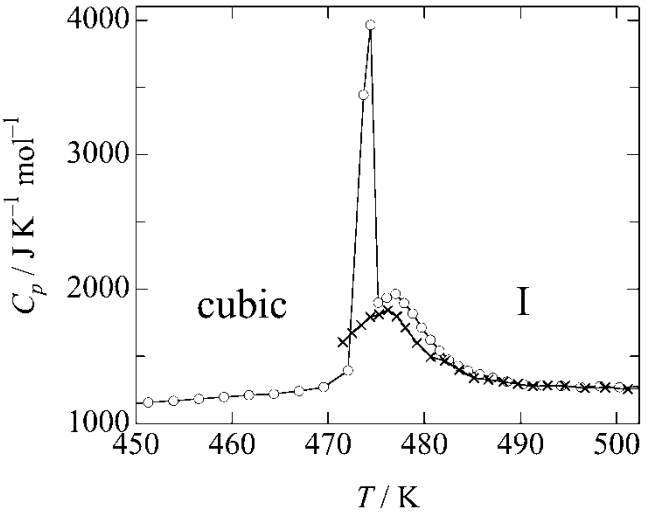

Figure 8. Heat capacities around the cubic–I transition of ACBC(16). Crosses show the result after cooling from the I phase to slightly below the transition temperature.

destruction of a higher order structure, and the possibility of the assignment of the hump to the destruction of shorter range order than that of the original length has been suggested [34]. Similar humps have been widely observed also in the analogous series, ANBC(n) [14]. Moreover, in the study on the binary system composed of ANBC and n-tetradecane [1], we reported the growth of the hump on increasing the paraffinic carbon atoms in the binary systems which do not exhibit any cubic phases. This observation was interpreted by assuming that the hump is due to the dissociation of ANBC dimers and that the growth originates in an entropy effect. The hump seen for ANBC(16) could be basically explained as the result of dissociation of carboxylic acid dimers formed in the crystalline and liquid crystalline phases, based on the experimental temperature dependence of the fraction of dimer by IR spectroscopy [3, 16]. There is no evidence that the ACBC molecules dimerize in the crystalline and liquid crystalline states. However, the similarity of the shape of the hump and the enthalpy involved—$4.4\,kJ\,mol^{-1}$ in comparison with $4.6\,kJ\,mol^{-1}$ in ANBC(16) [3]—strongly suggests that the hump in ACBC(16) is also related to the dissociation of carboxylic dimers, although the possibilities of the presence of a sluggish phase transition that the I phase undergoes, or the mechanism that the short range order is cooperatively destroyed in the I phase [34], cannot be omitted.

If the dissociation mechanism is assumed, then the following discussion can be made. The hysteresis observed in the DSC experiments implies that the dimerization equilibrium is a rather slow process. Its

time scale should be comparable to that of cooling in DSC experiments. A more interesting point is that a given fraction of the dimer is necessary for the formation of the cubic phase on cooling. The structural model involving two TPMSs proposed by ourselves (figure 2) [25] requires the two-side symmetry of the sheet [26] formed by the lateral intermolecular interactions. On the other hand, the sheet-type aggregation of dimers (the long axis being perpendicular to the sheet) automatically guarantees the two-side symmetry. The behaviour that two (sharp and broad) anomalies appear as a set even on cooling is, therefore, consistent with the structural model [25].

3.6. *Glass transition in the solid phase crystallized from the SmC phase*

While the heat capacity of the solid crystallized from the SmC phase has slightly smaller values between 50 and 155 K than that of the as-grown sample, it becomes larger in a step-wise manner at around 170 K and remains larger at higher temperatures as shown in figure 4. The data in this region are shown on an enlarged scale in figure 9. The step in the heat capacity is $60\,J\,K^{-1}\,mol^{-1}$. Around 165 K a gradual temperature increase began to be observed. A step in the heat capacity is characteristic of a glass transition, below which the system is not in thermodynamic equilibrium due to a prolonged relaxation time of some degree(s) of freedom [35]. The 'enthalpy relaxation' is also a characteristics of a glass transition and causes a temperature increase below (decrease above) the glass transition temperature. The behaviour of this solid crystallized from the SmC phase is, therefore, attributed to a glass transition. As the present compound has no degrees of freedom possibly excited at this temperature other than motional (structural) ones, the sample below this glass transition temperature ($T_g \approx 170$ K) will have some frozen-in structural disorder. Structural information is necessary to analyse the present result and in order to discuss further this solid phase crystallized from the SmC phase.

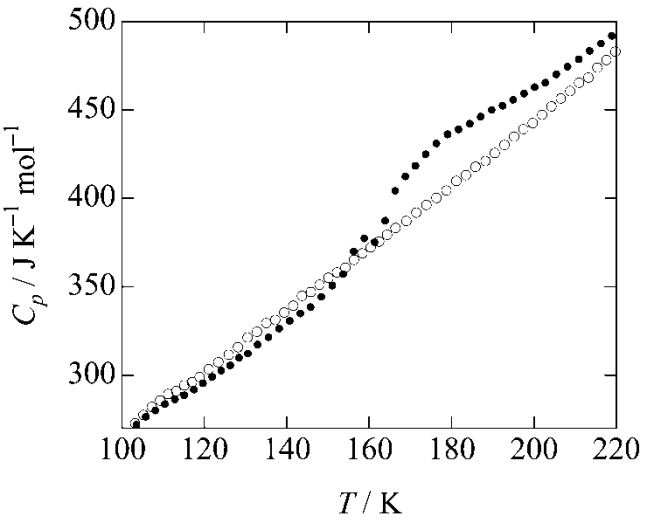

Figure 9. Heat capacities around the glass transition of ACBC(16) crystallized from the SmC phase (closed circles). The data of the as-grown sample are also shown for comparison by open circles.

4. Conclusion

The heat capacity of the optically isotropic mesogen ACBC(16) has been measured. The first order nature of the SmC – cubic phase transition at 431.15 K was confirmed for the first time by the observation of supercooling. The entropy of this transition ($\Delta_{trs}S = 2.67\,J\,K^{-1}\,mol^{-1}$) is larger than for ANBC(16) ($1.63\,J\,K^{-1}\,mol^{-1}$) for which the cubic phase is characterized by the space group *Ia*3*d*. The suppressed fluctuation in the cubic phase was detected as a smaller heat capacity than for the neighbouring liquid crystalline (SmC) phase. A broad hump in the heat capacity curve above the transition to the isotropic liquid at 474.30 K has been shown to extend to a low temperature side if the isotropic liquid is supercooled. This successful 'supercooling' of the hump is consistent with the dissociation of carboxylic dimers as a possible origin of the hump. These experimental results are discussed in respect to the structural model of the thermotropic cubic mesophases proposed by ourselves.

This work was supported in part by a Grant-in-Aid for Scientific Research (A) 11304050 from the Ministry of Education, Culture, Sports, Science, and Technology, Japan. One of the authors (M.S.) would like to acknowledge the Alarich and Elisabeth Weiss Fellowship, using which he visited Germany and initiated this collaboration. Two of the authors (Y.G. and I.G.) acknowledge the cooperative collaboration grants DLR RUS-00/203 and DFG 436 RUS 113/401/0. The authors are grateful to Prof. Shoichi Kutsumizu at Gifu University for useful discussions.

References

[1] Saito, K., Sato, A., and Sorai, M., 1998, *Liq. Cryst.*, **25,** 525.
[2] Morimoto, N., Saito, K., Morita, Y., Nakasuji, K., and Sorai, M., 1999, *Liq. Cryst.*, **26,** 219.
[3] Sato, A., Saito, K., and Sorai, M., 1999, *Liq. Cryst.*, **26,** 341.
[4] Sato, A., Yamamura, Y., Saito, K., and Sorai, M., 1999, *Liq. Cryst.*, **26,** 1185.
[5] Saito, K., Shinhara, T., and Sorai, M., 2000, *Liq. Cryst.*, **27,** 1555.

[6] SAITO, K., SHINHARA, T., NAKAMOTO, T., KUTSUMIZU, S., YANO, S., and SORAI, M., 2001, *Phys. Rev. E*, **65,** 031719.
[7] SORAI, M., and SAITO, K., 2003, *Chem. Rec.*, **3,** 29.
[8] GRAY, G. W., and GOODBY, J. W., 1984, *Smectic Liquid Crystals – Textures and Structures* (Glasgow and London: Leonard Hill), Chap. 4.
[9] GRAY, G. W., JONES, B., and MARSON, F., 1957, *J. chem. Soc.*, 393.
[10] DEMUS, D., KUNICKE, G., NEELSEN, J., and SACKMANN, H., 1968, *Z. Naturforsch.*, **23,** 84.
[11] SCHUBERT, H., HAUSCHILD, J., DEMUS, D., and HOFFMANN, S., 1978, *Z. Chem.*, **18,** 256.
[12] DEMUS, D., GLOZA, A., HARTUNG, H., HAUSER, A., RAPTHEL, I., and WIEGELEBEN, A., 1981, *Cryst. Res. Technol.*, **16,** 1445.
[13] UKLEJA, P., SIATKOWSKI, R. E., and NEUBERT, M., 1988, *Phys. Rev. A*, **38,** 4815.
[14] KUTSUMIZU, S., YAMADA, M., and YANO, S., 1994, *Liq. Cryst.*, **16,** 1109.
[15] LEVELUT, A.-M., and CLERC, M., 1998, *Liq. Cryst.*, **24,** 105.
[16] KUTSUMIZU, S., KATO, R., YAMADA, M., and YANO, S., 1998, *J. phys. Chem. B*, **101,** 10666.
[17] KUTSUMIZU, S., ICHIKAWA, T., YANO, S., and NOJIMA, S., 1999, *Chem. Commun.*, 1181.
[18] KUTSUMIZU, S., ICHIKAWA, T., YAMADA, M., NOJIMA, S., and YANO, S., 1999, *J. phys. Chem. B*, **104,** 10196.
[19] MAEDA, Y., CHENG, G.-P., KUTSUMIZU, S., and YANO, S., 2001, *Liq. Cryst.*, **28,** 1785.
[20] KUTSUMIZU, S., MORITA, K., ICHIKAWA, T., YANO, S., NOJIMA, S., and YAMAGUCHI, T., 2002, *Liq. Cryst.*, **29,** 1447.
[21] KUTSUMIZU, S., MORITA, K., YANO, S., and NOJIMA, S., 2002, *Liq. Cryst.*, **29,** 1459.
[22] GÖRING, P., DIELE, S., FISCHER, S., WIEGELEBEN, A., PELZL, G., STEGEMEYER, H., and THYEN, W., 1998, *Liq. Cryst.*, **25,** 467.
[23] ETHERINGTON, G., LEADBETTER, A. J., WANG, X. J., GRAY, G. W., and TAJBAKHSH, A., 1986, *Liq. Cryst.*, **1,** 209.
[24] ETHERINGTON, G., LANGLEY, A. J., LEADBETTER, A. J., and WANG, X. J., 1988, *Liq. Cryst.*, **3,** 155.
[25] SAITO, K., and SORAI, M., 2002, *Chem. Phys. Lett.*, **366,** 56.
[26] HYDE, S., ANDERSSON, S., LARSSON, K., BLUM, Z., LANDAH, T., LIDIN, S., and NINHAM, B. W., 1997, *The Language of Shape* (Amsterdam: Elsevier).
[27] OLAH, G. A., and KEUMI, T., 1979, *Synthesis*, **3,** 112.
[28] SUZUKI, A., 1994, *Pure appl. Chem.*, **66,** 213.
[29] SORAI, M., KAJI, K., and KANEKO, Y., 1992, *J. chem. Thermodyn.*, **24,** 167.
[30] SORAI, M., and SEKI, S., 1972, *J. phys. Soc. Jpn.*, **32,** 382.
[31] NISHIZAWA, M., SAITO, K., and SORAI, M., 2001, *J. phys. Chem. B*, **105,** 2987.
[32] SAITO, K., IKEDA, M., and SORAI, M., 2002, *J. therm. Anal. Calor.*, **70,** 345.
[33] KUTSUMIZU, S., *et al.*, unpublished results.
[34] GOODBY, J. W., DUNMUR, D. A., and COLLINGS, P. J., 1995, *Liq. Cryst.*, **19,** 703.
[35] SUGA, H., and SEKI, S., 1974, *J. non-cryst. Solids*, **16,** 171.